NAVAL POSTGRADUATE SCHOOL

MONTEREY, CALIFORNIA

THESIS

OPTIMIZING ENERGY EFFICIENT UAV ROUTING IN SUPPORT OF MARINE CORPS EXPEDITIONARY ADVANCED BASE OPERATIONS

by

Adam Jatho

June 2020

Thesis Advisor:	Vladimir N. Dobrokhodov
Second Reader:	Emily M. Craparo

THIS PAGE INTENTIONALLY LEFT BLANK

REPORT DOCUMENTATION PAGE			*Form Approved OMB No. 0704-0188*

1. AGENCY USE ONLY *(Leave blank)*	**2. REPORT DATE** June 2020	**3. REPORT TYPE AND DATES COVERED** Master's thesis

4. TITLE AND SUBTITLE OPTIMIZING ENERGY EFFICIENT UAV ROUTING IN SUPPORT OF MARINE CORPS EXPEDITIONARY ADVANCED BASE OPERATIONS	**5. FUNDING NUMBERS**
6. AUTHOR(S) Adam Jatho	
7. PERFORMING ORGANIZATION NAME(S) AND ADDRESS(ES) Naval Postgraduate School Monterey, CA 93943-5000	**8. PERFORMING ORGANIZATION REPORT NUMBER**
9. SPONSORING / MONITORING AGENCY NAME(S) AND ADDRESS(ES) N/A	**10. SPONSORING / MONITORING AGENCY REPORT NUMBER**

11. SUPPLEMENTARY NOTES The views expressed in this thesis are those of the author and do not reflect the official policy or position of the Department of Defense or the U.S. Government.

12a. DISTRIBUTION / AVAILABILITY STATEMENT Approved for public release. Distribution is unlimited.	**12b. DISTRIBUTION CODE** A

13. ABSTRACT (maximum 200 words)

Resupplying future United States Marine Corps' expeditionary advanced bases means developing resilient resupply methods. This thesis looks for a solution to reduce the risks associated with complex resupply operations, where troops and high-value equipment are exposed to the dangers of operations in a contested environment. Using unmanned aerial vehicles (UAVs), logistics missions can be conducted at greater efficiency and at lower risk to the force. This work addresses the problem of last-mile resupply using multiple autonomous UAVs. We develop an optimal UAV routing system, which creates the optimal energy-efficient flight paths for the UAVs between resupply nodes, accounting for changing wind conditions. The optimal minimum energy-trajectory generation (UAV flight path and velocity along the flight path) that connects each pair of nodes is based on the Pontryagin maximum principle. By minimizing energy expenditures required for flight, we increase UAV range and decrease the logistical resupply footprint in contested terrain. In order to minimize energy expenditures among multiple resupply nodes, we build on work done with a multiple-traveling salesmen problem to create optimal UAV delivery routes. While the general case of the optimal routing problem is not new, formulating this task as an optimal trajectory control problem, tied to the optimal routing of military logistics missions, increases the flexibility, agility and effectiveness of the Marine Corps.

14. SUBJECT TERMS optimal control, optimal routing, UAV, UAV routing, logistics	**15. NUMBER OF PAGES** 61
	16. PRICE CODE

17. SECURITY CLASSIFICATION OF REPORT	**18. SECURITY CLASSIFICATION OF THIS PAGE**	**19. SECURITY CLASSIFICATION OF ABSTRACT**	**20. LIMITATION OF ABSTRACT**
Unclassified	Unclassified	Unclassified	UU

NSN 7540-01-280-5500

Standard Form 298 (Rev. 2-89)
Prescribed by ANSI Std. 239-18

THIS PAGE INTENTIONALLY LEFT BLANK

Approved for public release. Distribution is unlimited.

OPTIMIZING ENERGY EFFICIENT UAV ROUTING IN SUPPORT OF MARINE CORPS EXPEDITIONARY ADVANCED BASE OPERATIONS

Adam Jatho
Captain, United States Marine Corps
BS, U.S. Naval Academy, 2014

Submitted in partial fulfillment of the
requirements for the degree of

MASTER OF SCIENCE IN OPERATIONS RESEARCH

from the

NAVAL POSTGRADUATE SCHOOL
June 2020

Approved by: Vladimir N. Dobrokhodov
Advisor

Emily M. Craparo
Second Reader

W. Matthew Carlyle
Chair, Department of Operations Research

THIS PAGE INTENTIONALLY LEFT BLANK

ABSTRACT

Resupplying future United States Marine Corps' expeditionary advanced bases means developing resilient resupply methods. This thesis looks for a solution to reduce the risks associated with complex resupply operations, where troops and high-value equipment are exposed to the dangers of operations in a contested environment. Using unmanned aerial vehicles (UAVs), logistics missions can be conducted at greater efficiency and at lower risk to the force. This work addresses the problem of last-mile resupply using multiple autonomous UAVs. We develop an optimal UAV routing system, which creates the optimal energy-efficient flight paths for the UAVs between resupply nodes, accounting for changing wind conditions. The optimal minimum energy-trajectory generation (UAV flight path and velocity along the flight path) that connects each pair of nodes is based on the Pontryagin maximum principle. By minimizing energy expenditures required for flight, we increase UAV range and decrease the logistical resupply footprint in contested terrain. In order to minimize energy expenditures among multiple resupply nodes, we build on work done with a multiple-traveling salesmen problem to create optimal UAV delivery routes. While the general case of the optimal routing problem is not new, formulating this task as an optimal trajectory control problem, tied to the optimal routing of military logistics missions, increases the flexibility, agility and effectiveness of the Marine Corps.

THIS PAGE INTENTIONALLY LEFT BLANK

Table of Contents

THIS PAGE INTENTIONALLY LEFT BLANK

List of Figures

List of Acronyms and Abbreviations

BVP	boundary value problem
CBC	Computational Infrastructure for Operations Research branch and cut
COAMPS	Coupled Ocean/Atmosphere Mesoscale Prediction System
EABO	Expeditionary Advanced Base Operations
EXLOG	Expeditionary Logistics
ISR	intelligence, surveillance, and reconnaissance
LOCE	Littoral Operations in a Contested Environment
MAGTF	Marine Air-Ground Task Force
MILP	mixed-integer linear program
mTSP	multiple-traveling salesman problem
PMP	Pontryagin's maximum principle
UAV	unmanned aerial vehicle
VRP	vehicle routing problem

THIS PAGE INTENTIONALLY LEFT BLANK

Executive Summary

In a future fight against a near-peer enemy, the Marine Corps cannot count on uncontested resupply lines of communication to supply distributed forces. As Marines seek to establish expeditionary bases in hostile terrain, they must also identify novel ways to keep those bases supplied with the food, fuel, and ammunition to win the battle.

This thesis looks for a solution that reduces the risk to Marines and equipment typically associated with complex resupply operations. Using autonomous UAVs, logistics missions can be conducted at greater efficiency and at lower risk to the Marines on the ground. We develop an optimal unmanned aerial vehicle routing system, which creates energy-efficient flight paths for UAVs between resupply nodes, accounting for real-world weather conditions, before optimizing overall resupply routes across demand nodes.

Our method builds energy optimal trajectories (UAV flight path and velocity along the arc from node i to node j) that connect each pair of nodes and is based on Pontryagin's maximum principle (PMP). We show that wind has a large impact on these optimal trajectories, in certain cases even making routes impassable. Figure 1 demonstrates potential UAV energy savings of 70 percent depending on the direction of travel along the arc. Without taking wind into account, and simply using great circle distance to calculate costs between delivery locations, we ignore a critical component of energy expenditure calculations.

```
(13, 15) : 27602.66
(15, 13) :  8454.72
```

Figure 1. The Actual Energy Cost, (Wh) Depending on Direction of Travel, Along the Arc from Node 13 to Node 15

In order to minimize energy expenditures over the duration of resupply missions, we build on optimization work done with the mixed-integer linear program (MILP) multiple-traveling salesmen problem to create optimal UAV delivery paths from a single supply depot, to multiple delivery locations prioritized by need, and back to the supply depot. Optimal routing of UAVs across the resupply nodes further decreased energy expenditures by between 2.5 and 11 percent.

This thesis shows the value of using real-world wind when identifying the cost matrix for resupply routes. Combining this realistic data with a routing system based on the multiple-traveling salesman problem yields energy-efficient routing results that would not be evident to a task saturated Marine logistician in the field. These optimal routing results save energy, energy that can be used to increase UAV range, carry more supplies, and limit the energy burden at supply depots far from America's shores.

Acknowledgments

Thank you to my advisor, Dr. Vladimir Dobrokhodov, who was instrumental in helping me throughout the thesis process.

I would also like to thank my second reader, Dr. Emily Craparo, for her teaching and for helping me work through the model formulation and review process.

Finally, thank you to my wife, Bizzie, for always supporting me.

THIS PAGE INTENTIONALLY LEFT BLANK

CHAPTER 1:
Introduction

> We cannot meet the demands of an agile, distributed 21st century Marine Air-Ground Task Force Marine Air-Ground Task Force (MAGTF) with a 20th century approach to logistics. Our logistics enterprise has to provide expeditionary support and sustainment from the greater distances imposed by A2AD threats. It must accommodate the threat from increasingly capable intelligence, surveillance, and reconnaissance (ISR)-strike capabilities to the viability of large, fixed-site support facilities. It must be capable of supporting distributed units on a widely dispersed battlefield and reduce the burden that must be carried by the individual Marine...Expeditionary Logistics (EXLOG) will require a maneuver warfare mindset. EXLOG must be responsive, agile, and resilient to support and sustain operations on the move in austere environments and frequently on short notice. (MOC, 2016, p. 23)

As "China seeks to displace the United States in the Indo-Pacific region" (NSS, 2017, p. 25) Marines will increasingly be called upon to conduct operations in constricted island terrain. These operations, collectively referred to as "Littoral Operations in a Contested Environment (LOCE)," present a challenge to a Marine Corps used to conducting counter-terrorism operations from static bases. In a region where ballistic missiles, drones, and people proliferate, the Marine Corps will be forced to embrace a new strategy in order to thrive and win. One such strategy is setting up dispersed expeditionary advanced bases. By dispersing forces across expeditionary bases, we "maintain a forward military presence capable of deterring and, if necessary, defeating any adversary" (NSS, 2017, p. 47). These expeditionary advanced bases support sea control through their offensive capabilities and defensive staying power in a contested littoral environment.

This new strategy relies on small-scale dispersed forces. These forces will require flexible logistics support systems which can support them in a contested environment. Traditional resupply methods like port and convoy operations produce too large a signature and in turn become too easy to target. The new resupply system needs to be scalable, robust, autonomous, and redundant in order to safely provide distributed forces the food, fuel, and ammunition to fight. One promising method to do this is through a network of supply

depots which provide autonomous unmanned aerial vehicles (UAVs, also known as drones) enabling low-cost resupply missions to the dispersed force (compared to manned helicopters or ships). These forward-deployed logistical bases can provide "temporary forward and intermediate staging areas for MAGTF follow-on echelons and sustainment operations" (MOC, 2016, p. 13). By developing resupply capabilities with unmanned drones, we can support bases with a smaller footprint that can operate within enemy or contested territory. This support enables Marines at difficult-to-dislodge outposts to stay in the fight and conduct offensive operations.

Supporting future United States Marine Corps' Expeditionary Advanced Base Operations (EABO) means developing an optimal UAV routing system that takes advantage of current and future UAV technology by creating the energy-optimal flight paths for the UAVs.

By minimizing energy expenditures required for flight, we decrease charging and battery requirements, increase UAV range, and decrease the logistical resupply footprint in contested terrain. In order to minimize energy consumption, UAVs must have efficient routing and flight plans. These two plans, based on weather forecasts with an emphasis on wind, are critical to resupplying dispersed forces as they conduct operations in any contested environment.

In the commercial world, the "last mile" of deliveries is often a key focus since movement between large warehouses is relatively simple compared to navigating a city with hundreds of thousands of addresses in order to fulfill orders. Marines must not only navigate unfamiliar and potentially hostile terrain, but must also remain concealed from the enemy. For the logistician, this presents additional last-mile challenges with a continuously developing set of limitations, constraints, and demands. An automated optimal routing system is part of the solution.

This thesis combines two optimization approaches, first developing a realistic cost matrix using mesoscale wind and elevation data, then feeding that data into a routing model that solves for the optimal UAV flight paths.

To develop the cost matrix, wind energy characterization along with the list of desired destinations are fed into a boundary value problem solver which creates energy-optimal UAV flight segments between logistics depots and requesting delivery nodes. These segments,

and the associated energy expenditure by UAVs that fly them, are fed into a route optimization model, based on the multiple traveling salesman problem, which solves for the optimal routing for all UAVs. With the ability to recalculate the routes based on changing wind conditions, this model's inherent flexibility provides Marines with robust resupply options using low-cost UAVs.

THIS PAGE INTENTIONALLY LEFT BLANK

CHAPTER 2:
Background

2.1 Combinatorial Optimization

When considering an optimization problem, clearly it is desirable to find the globally optimal solution. For some problems, however, the time required to find such a solution is excessive.

The EABO unmanned aerial vehicle (UAV) routing problem is grounded in the reality of last-mile logistics in support of a MAGTF where it is reasonable to assume that there will be no more than 50 demand nodes. Therefore, a mixed-integer linear program can be solved to near-optimality within a matter of minutes using the Computational Infrastructure for Operations Research branch and cut (CBC) solver which solves a model built using Pyomo modeling software (Hart et al. (2017) and Hart, Watson, and Woodruff (2011)). Other solutions that solve problems with a larger number of nodes require heuristics, which do not provide optimality guarantees.

By using a mixed-integer linear program (MILP) approach, we can solve for the true optimal solution. If the problem does become too large, we can implement a control which provides a solution that is within 10 percent proximity of optimal, but solves much faster.

Our problem is based on the multiple-traveling salesman problem, and is formulated using mixed-integer linear programming. Mixed-integer linear programming combines linear, integer, and binary constraints. In our case, the main binary decision variable is whether or not UAV k travels along arc X_{ij} and is represented by either a 1 or a 0.

2.2 The Traveling Salesman Problem

The traveling salesman problem is one of the fundamental problems in combinatorial optimization. In the traveling salesman problem, a graph G consists of n nodes representing destination cities and X_{ij} arcs representing possible routes from city i to city j.

The problem is to find the the minimum-distance route that a salesman, who is seeking to

go from his depot (or starting node) to every other node before returning to the depot, can travel. It is important to note that the depot node is represented as node 1 within the set of nodes (1, n).

Because of the inherent combinatorial complexity (NP hard) of the problem, a universally optimal solving method does not exist and specific methods are chosen based on their ability to solve specific problems. An exhaustive search for the optimal solution is possible, but can take a long time if the number of possible paths through the graph are large.

For our problem with a limited number of nodes to serve, we chose a mixed-integer linear programming model which can be solved to optimal or near-optimal conditions. Our solution is based on the Miller, Tucker, and Zemlin (1960) formulation of the TSP:

$$\min \sum_{i=1}^{n} \sum_{j \neq i, j=1}^{n} C_{ij} X_{ij} \tag{2.1}$$

$$\sum_{j=1}^{n} X_{1j} = 1 \tag{2.2}$$

$$\sum_{i=1}^{n} X_{i1} = 1 \tag{2.3}$$

$$\sum_{i=1}^{n} X_{ij} = 1 \qquad j = 2, \ldots, n \tag{2.4}$$

$$\sum_{j=1}^{n} X_{ij} = 1 \qquad i = 2, \ldots, n \tag{2.5}$$

$$u_j - u_i \geq 1 - (n-1)(1 - X_{ij}) \qquad \forall i, \forall 2 \leq j \leq n, j \neq i \tag{2.6}$$

$$u_1 = 1 \tag{2.7}$$

$$2 \leq u_j \leq n \qquad j = 2, \ldots, n \tag{2.8}$$

$$u_j \quad \text{integer} \qquad j = 2, \ldots, n \tag{2.9}$$

$$X_{ij} \in \{0, 1\} \qquad \forall i, j \tag{2.10}$$

Where X_{ij} (2.10) is the binary decision variable denoting whether or not the salesman

travelled from node i to node j and C_{ij} represents the cost to travel from node i to node j (the depot node is node 1).

The objective function 2.1 computes the salesman's total travel distance by multiplying the cost matrix C_{ij} by the binary variable X_{ij}, and seeks to minimize distance travelled by the salesman. The variable u_i is used in a constraint to ensure that degenerate subtours do not exist.

Constraints 2.2 and 2.3 ensure that the salesman departs and arrives back at the depot node only once. Constraints 2.4 and 2.5 ensure that the salesman enters and exits each destination node only once. Constraints 2.6-2.9 form the family of Miller-Tucker-Zemlin subtour-elimination constraints, preventing disconnected cycles from appearing in a salesman's route by ensuring that every cycle contains the depot node.

2.2.1 The Multiple-Traveling Salesman Problem

The multiple-traveling salesman problem (mTSP) is a generalization of the TSP problem with multiple salesman, m. With only one salesman, the mTSP reduces to the TSP. Without capacity constraints, limits on the salesman's ability to service a certain number of nodes, or travel a certain distance, the optimal solution is always identical to the TSP, with one salesman making the tour in order to minimize spent cost or distance travelled.

$$\min \sum_{i=1}^{n} \sum_{j\neq i,j=1}^{n} \sum_{k=1}^{m} C_{ij} X_{ijk} : \tag{2.11}$$

$$\sum_{j=2}^{n} X_{1jk} = 1 \qquad \forall\ k \in \{1,...m\} \tag{2.12}$$

$$\sum_{i=2}^{n} X_{i1k} = 1 \qquad \forall\ k \in \{1,...m\} \tag{2.13}$$

$$\sum_{j=1}^{n} \sum_{k=1}^{m} X_{ijk} = 1 \qquad \forall\ i \in \{2,...n\} \tag{2.14}$$

$$\sum_{i=1}^{n} \sum_{k=1}^{m} X_{ijk} = 1 \qquad \forall\ j \in \{2,...n\} \tag{2.15}$$

$$\sum_{i=1}^{n} X_{irk} = \sum_{j=1}^{n} X_{rjk} \qquad \forall\ r \in \{2,...n\} \quad \forall\ k \in \{1,...m\} \tag{2.16}$$

$$u_i - u_j + (n-m) * \sum_{k=1}^{m} X_{ijk} \leq n - m - 1 \qquad \forall\ i,j \in \{2,...n\} \quad \forall\ k \in \{1,...m\} \tag{2.17}$$

$$X_{ijk} \in \{0,1\} \qquad \forall i,j \tag{2.18}$$

$$u_i \in \{\mathbb{Z}\} \qquad \forall i \in \{2,...n\} \tag{2.19}$$

This reformulation from Y. Kaempfer et al. (Kaempfer and Wolf (2019)) adds an additional dimension k to X_{ij}. k refers to the salesman who makes the trip along arc X_{ij}. m refers to the the total number of salesmen available to complete the tour of all nodes within the graph. This allows salesmen to be indexed from 1 to m within the model. The addition of constraint 2.16 ensures that the each salesman enters and exits every node only once, thereby conserving salesman flow within the graph and preventing multiple salesmen from visiting the same node i.

2.3 Vehicle Routing Problem

The vehicle routing problem (VRP) is a variation of the mTSP with additional constraints modeling node demands, vehicle capacity constraints, demand time windows, and delivery vehicle selection (Cheng, Adulyasak, and Rousseau (2018)). Dorling et al. propose two

models: one to minimize delivery cost and the other to minimize delivery time within a certain budget (Dorling, Heinrichs, Messier, and Magierowski (2016)). Our problem uses energy and time as the cost interchangeably.

Other research by Jaillet and Lu Jaillet and Lu (2011) focuses on increasing the flexibility of the problem by introducing penalties for missing certain nodes and increasing flexibility in scheduling during the execution of a "tour." With a problem that is "offline," the nodes n are set before traveler departs. An "online" problem can have additional nodes added or dropped during the mission. They address the added complexity of this problem by adding penalty values for each node, so that if some nodes are skipped this leads to increased penalty on the objective function.

2.3.1 Scheduling

Our problem focuses on minimizing total energy associated with the travel in order to address energy consumption and uses demand priorities to ensure important customers are guaranteed support. Specific time windows, by demand node, are beyond the scope of our current problem.

The traveling salesman problem with time windows is a subset of the traveling salesman problem that incorporates time windows into delivery node information. Parallels with our work routing UAVs can be drawn from prior research optimizing helicopter logistics. Linet Ozdamar's work on optimal helicopter routing delivering aid after natural disasters can be adapted to UAVs (Ozdamar (2011)) in future work.

2.3.2 Resource Constraints

Modern UAVs belong to two categories: quadrotors, which are effective "lifters" but poor long-distance fliers, and fixed-wing aircraft, which are efficient in long distance flights but require long runways for heavy load lifting. At the initial stage of task formulation, and when building a computational framework, we adopt a generic UAV model that is representative of energy expenditures associated with flight and include real-world wind.

Since drone technology is continuously evolving, we approached lift capacity from a holistic approach and allow the user to provide lift capacity as an data input, by specific UAV k.

This allows the model to solve for instances with a variety of different lift capacities.

We did not address the packing problem, which seeks to most efficiently pack specific supply items into a UAV for more balanced flight or shorter delivery service times on the ground. Our model uses unitless supply and demand values to account for the carrying capacity of the UAVs.

2.4 Optimal Control in Flight

Unlike a traditional VRP with ground vehicles, UAV delivery introduces an entirely new element: flight. With flight comes a three-dimensional flight path with six possible flight directions as well as an associated airspeed. Previous research can be divided into two areas of focus: UAV optimal flight paths and optimal flight trajectories with wind as a consideration; trajectory is represented by the path and the velocity profile associated with that path. Optimal trajectory generation is the task of finding the path and the velocity profile along the path that minimize a chosen cost together. The choice of cost depends on the trajectory planning objectives and the type of the autonomous vehicles. One commonality among the various types of UAVs is the general dependence on the capacity of onboard energy sources (batteries, fuel, or fuel cells). While the energy is always constrained, the approach we envision is to use what is given onboard while minimizing unnecessary "fight" with environmental effects like wind and terrain. Thus the objective of the single trajectory optimization problem is to minimize the waste of onboard limited energy resources by maximizing the use of environmental energy, also known as energy-aware trajectory optimization.

In our problem, we focus on UAV multicopters that have very specific energy expenditures in different stages of flight. Research by Liu, Sengupta, and Kruzhanskiy into optimal control of the UAV from the consideration of energy efficiency focuses on three different types of energy expenditures: induced, profile, and parasite power (Liu, Sengupta, and Kurzhanskiy (2017)). Induced power refers to the power expended to keep the UAV airborne, profile is the power required to keep the UAV at a certain attitude angle, and parasitic power is the power penalty due to loss of energy by drag.

Previous work by Gil Nachmani focused on optimizing UAV flight paths by taking advantage of small scale wind forecasts (Nachmani (2007)). He found average energy savings of

approximately 30 percent when optimal trajectories were compared to straight, typical, shortest path routes through the air. When combined with node-to-node route optimization, there is a potential for even higher energy savings.

Flight path optimization draws on research on the boundary value problem (BVP), which is based on indirect optimization using the Pontryagin's maximum principle (PMP) (Pontryagin (1962)).

Research by Dobrokhodov, Jones, Walton, and Kaminer (2020) shows that it is possible to create more efficient flight paths (compared to great circle routes) to generate cost savings. Their research showed significant energy savings in long range UAVs using this method.

2.5 Solution Overview

Our approach combines the boundary value problem and an MILP vehicle routing problem (VRP) as two layers shown on the top of Figure 2.1 as the "route estimator" and the "VRP," respectively.

Demands are communicated from the Marines in the field back to a logistician who runs the routing program based on the demand nodes. The system takes these demands and creates possible flight paths from each node i to node j, taking wind into account and giving $n(n-1)$ possible flight arcs along which UAVs could travel. Layer one (the Route Estimator) takes the task formulation data (delivery demands and locations) and constraints and builds the asymmetric cost matrix with wind-based flight energy costs between demand nodes. This step is based on the indirect optimal control approach and implements the Pontryagin maximum principle. The second layer (VRP) utilizes a mixed-integer linear program that takes the cost matrix of the first layer as a data input and maximizes reward for completing deliveries to delivery nodes. The VRP also minimizes overall flight path cost, and solves for the optimal routing of UAVs to and from the depot.

In Figure 2.1, we show the communications network that we envision for a final product. In the future, we hope that the work in this thesis forms a basis for a program that can produce UAV routing flight paths based on real or simulated scenarios.

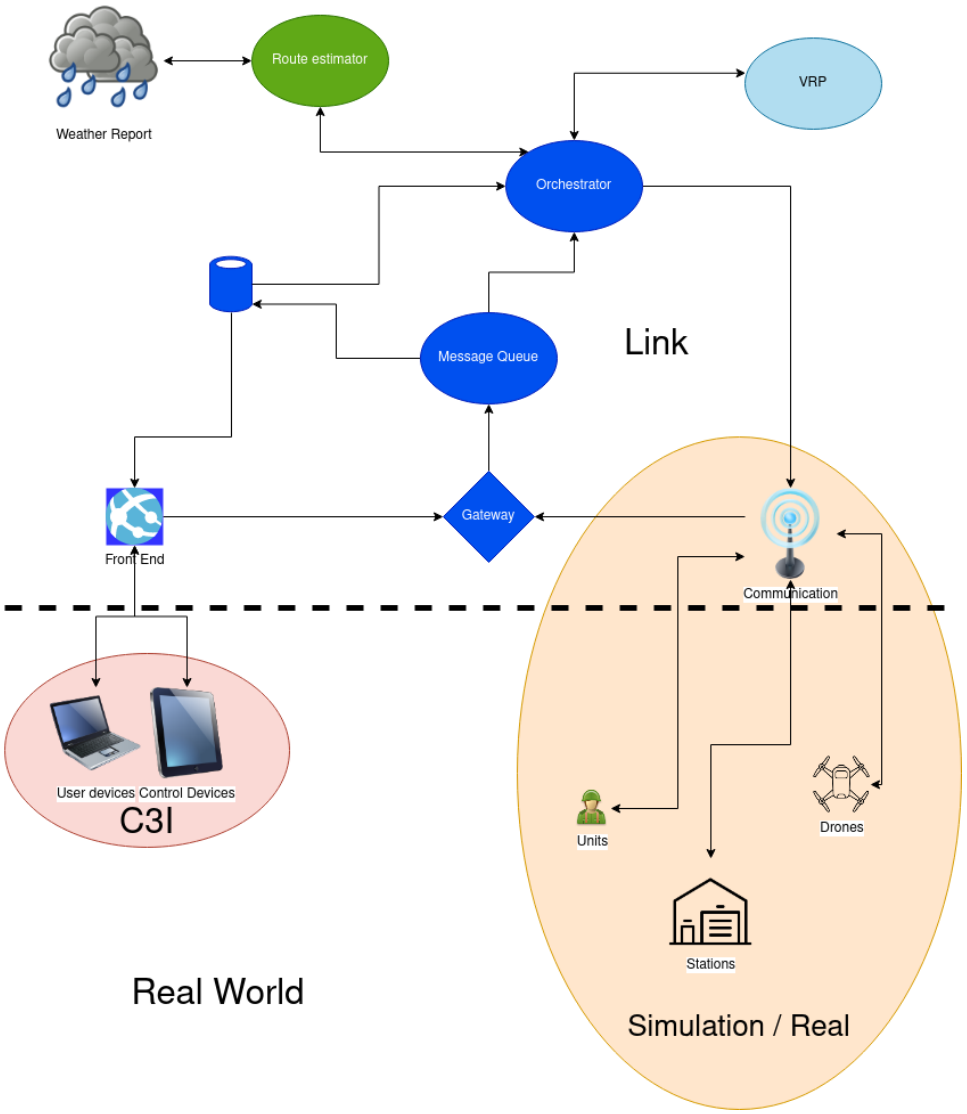

Figure 2.1. UAV Routing System Overview

2.6 Summary

By combining the vehicle routing problem and the boundary value problem, we seek to optimize not only the route between nodes, but also the flight path in order to decrease delivery times, limit UAV energy consumption in flight, and optimize delivery routes.

We save computation time by solving the boundary value problem more efficiently at the BVP solver layer by appropriate scaling of the Hamiltonian system and implementing a continuation algorithm that solves for an initial guess solution and provides the rapid

convergence characteristics of the indirect optimizer. The VRP problem remains NP-Hard, but due to the limited number of demand nodes, we are able solve it exhaustively.

THIS PAGE INTENTIONALLY LEFT BLANK

CHAPTER 3:
Flight Trajectory Optimization

This chapter describes a UAV flight trajectory optimization that is based on an indirect approach which is a foundation of optimal control. Specifically, it utilizes the PMP (Pontryagin (1962)) to build and solve the boundary value problem (BVP).

The task is to build a Hamiltonian system that explicitly accounts for the flight dynamics and the energy required to fly in an energy field (i.e., wind). The result of applying the PMP approach to this formulation is the optimal trajectory (comprised of the commanded flight path and the associated airspeed) and the associated energy metrics for each arc between nodes. When aggregated, these multiple segments become an asymmetric cost matrix that captures the energy cost required for flight between any node i to node j and is subsequently used in the UAV Routing Model.

3.1 Introduction

A UAV is an aircraft with an on-board autopilot that introduces a stability augmentation and guidance system (Driscoll (1967)). Despite the generally highly nonlinear dynamics of flight of airplanes of different configurations, the stability augmentation system makes the aircraft not only stable but also behave dynamically similar to a point mass that can be controlled, depending on the configuration, by the aircraft attitude (roll, pitch) and the throttle (airspeed) inputs. Thus, having an autopilot on board significantly simplifies the higher level trajectory optimization task because one no longer needs to consider a myriad of nonlinearities and constraints that complicate the formulation and solution of optimization tasks.

Bryson (1975) provides a demonstration of how the point mass model of a generic aircraft is used in a trajectory optimization task with the roll, pitch, and airspeed as control inputs. These three controls generate aerodynamics (meaning that they depend on the interaction of the aircraft with the surrounding air or fluid), forces, and moments that maneuver the UAV in flight and are highly susceptible to the effects of wind. It is easy to imagine a scenario where the UAV simply cannot progress along a certain path i, j due to a strong headwind.

An optimal flight trajectory is comprised of a path and the airspeed along the path. This path takes wind into consideration in order to guide the UAV from node i to node j in the most efficient way possible. Modeling wind on a two-dimensional plane, we can derive optimal flight controls based on wind's interactions with our three possible control inputs.

This method also allows us to model no-go areas (such as high mountains, enemy territory, or high-intensity weather storms) with a penalty value (Marinova (2012)) in the objective function in order to solve an optimization problem for the most energy-efficient flight path. This convex minimization problem, by virtue of PMP, solves for this efficient, and optimal, global minimum.

3.2 Formulation of the Optimal Control Problem

The optimal control problem seeks to minimize flight energy expenditures given certain real-world constraints with different penalties assigned to "no-go" areas, or areas where the weather conditions make flight impossible. We assume that each UAV has an autopilot system which enables steady state flight and removes our need to account for aircraft stability in flight.

We seek to minimize energy expenditures on the flight route by using optimal control of the aircraft heading and airspeed. By using a two dimensional plane to capture the major portion of flight while in optimal cruise mode, we can optimally traverse the plane. This problem has its roots in Pontraygin's maximum principle (Pontryagin (1962)). This principle states that in order to find an optimal solution for the optimal control problem between two locations (boundary points), given control inputs and power output constraints, one must solve the Hamiltonian boundary value problem (Pontryagin (1962)). Once solved, it satisfies the necessary conditions of optimality which become sufficient due to convexity.

3.2.1 Minimum Energy Optimal Control Task

Objective Function

The goal of this optimization task is to find the optimal airspeed (V) and bank angle (φ) inputs that minimize energy use over distance and time. For a typical fixed-wing UAV, this is calculated by integrating, by time, net power used by the UAV over the flight between the

initial and final point, shown in Equation 3.1. Power used depends on the state dynamics shown in Equations 3.2-3.6.

$$\min \int_{t_0}^{t_f} P_{net} dt \tag{3.1}$$

Subject to the following state dynamics:

$$\dot{x} = V \cos\psi + W_x(x, y, t) \tag{3.2}$$

$$\dot{y} = V \sin\psi + W_y(x, y, t) \tag{3.3}$$

$$\dot{\psi} = g \tan\varphi / V_g \tag{3.4}$$

$$V_g = \sqrt{\dot{x}^2 + \dot{y}^2} \tag{3.5}$$

$$\dot{\tau} = 1/t_f \tag{3.6}$$

These state dynamics are based on the fixed-wing UAV point-mass model on an x and y Cartesian plane, where V is airspeed, V_g is the ground speed of the UAV, and ψ is the ground heading angle. The wind is represented with W_x and W_y, which represent the direction of wind on the Cartesian coordinate system. The two control inputs, φ and V are the bank angle and commanded airspeed of the aircraft, respectively. Dynamic 3.6 is a way to represent the dimensionless progression along the path that is calculated with respect to initially unknown arrival time, t_f and is an optimization parameter of the boundary value problem solver.

In order to solve this system of differential equations, we must introduce a Hamiltonian function first discovered by Pontryagin (Pontryagin (1962)). The resulting Hamiltonian, Equation 3.7, is comprised of the drag model contribution via coefficients, $K_{p1,p2}$, and co-states ($\lambda_{x,y,\psi}$) associated with the state dynamics (Dynamics 3.2 - 3.6). Finally, the Hamiltonian is represented with respect to V and φ, which are the two control inputs to be solved for.

$$H = V^3 K_{p1} + K_{p2}/(V\cos^2\varphi) + \lambda_x \dot{x} + \lambda_y \dot{y} + \lambda_\psi \dot{\psi} \tag{3.7}$$

Due to non-autonomous nature of the wind dynamics, we know that at t_f the Hamiltonian will be equal to zero, which forms an additional boundary condition necessary to solve the system of equations. Combining the state and co-state dynamic equations with the two control inputs (airspeed: V and bank angle: φ), synthesised based on the first order necessary conditions (Dobrokhodov et al. (2020)), we can then solve for the optimal control inputs which produce an optimal flight from point i to point j, given wind conditions. These two optimal controls are shown in 3.8 and 3.9, which show the formulas for optimal bank angle and optimal airspeed, respectively.

$$\tan\varphi* = \frac{-V}{V_g}.\frac{\lambda_\psi g + V_g \dot{K}\cos e \sin(a-\psi)}{2K_{p2} + V\dot{K}_s \sin e} \tag{3.8}$$

$$V^{*2} = \sqrt{\frac{4K}{3\rho^2 C_{D_0}}(\frac{mg}{S})^2 + \frac{\eta_{prop}^2}{9\rho^2 S^2 C_{D_0}^2}\Lambda^2} - \frac{\eta_{prop}}{3\rho S C_{D_0}}\Lambda \tag{3.9}$$

3.3 Boundary Value Problem Implementation

Our solution has its basis in previous work by Dobrokhodov et al. (2020) who implemented the boundary value problem with long-range UAVs in order to develop optimal flight plans, and demonstrated the energy savings gained by using the approach. We use smaller-scale high-density weather maps and the same general approach to identify the optimal controls required to fly generic UAVs on smaller-scale resupply missions. These controls, when evaluated over the duration of the flight, account for the total energy costs over the route and form our cost matrix C_{ijk}.

The boundary value problem's implementation of object avoidance, shown in Figure 3.1 using MATLAB, shows the UAV flight path in turquoise around "no-go" zones represented by the red stars. Starting at the bottom of the graph and ending in the top right, we show that the use of a penalty function (a potential function) with increasing intensity (beginning

in the blue circle) causes the UAV's control function to bend the route shape, allowing the UAV to pass between two zones, and achieve an optimal point-to-point flight path.

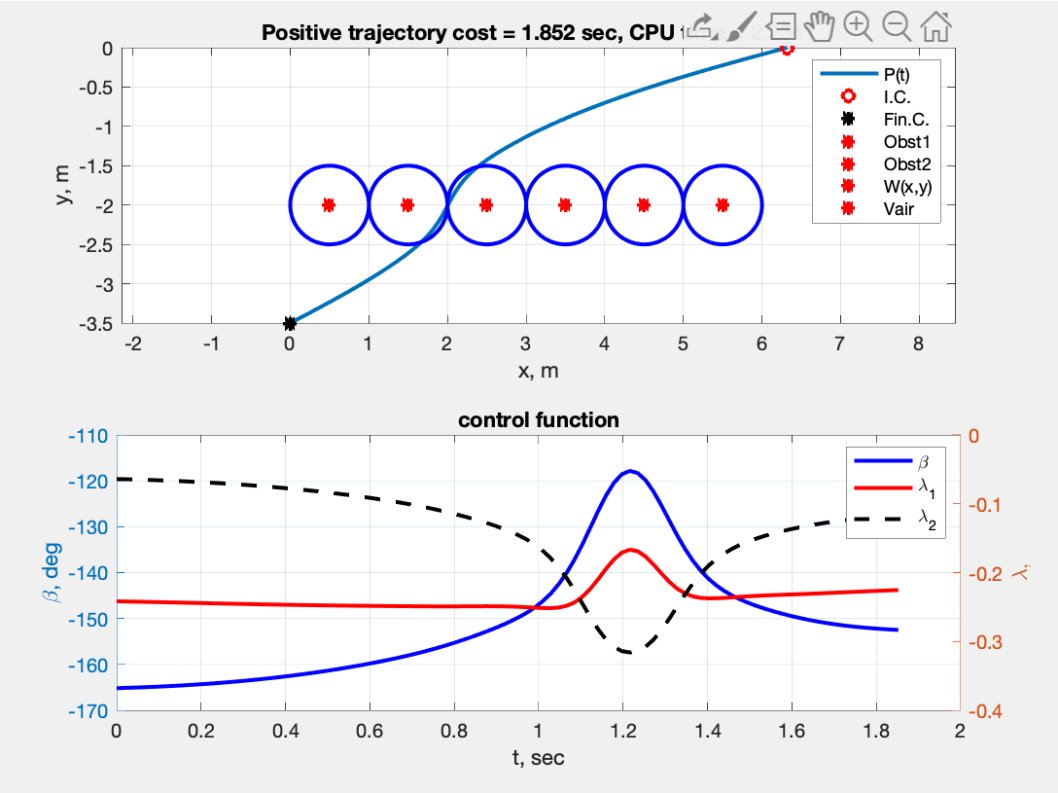

Figure 3.1. Boundary Value Problem Demonstrating Object Avoidance

3.3.1 Coupled Ocean/Atmosphere Mesoscale Prediction System

In order to develop accurate flight paths we use geographical data that is overlaid with a predicted wind forecast built using the Coupled Ocean/Atmosphere Mesoscale Prediction System (COAMPS) model developed by the U.S. Naval Research Laboratory (The Naval Research Laboratory (1997)). The COAMPS model produces wind forecasts with a specified spatial resolution depending on the range of the UAVs and dispersion of requesting delivery nodes. An example of the COAMPS wind forecast can be found in Figure 3.2, with wind represented by colored blocks and color denoting wind direction and intensity.

3.3.2 Wind Scaling and Implementation

To efficiently and rapidly solve the boundary value problem numerically, we iterate through different scales of wind, beginning with a wind scale of $1/1000$ and working down to a $1/1$ scale (representing the most detailed wind that the COAMPS data provides) using the COAMPS wind data. This "continuation" method solves the problem with an initial guess and creates an optimal flight path by decreasing the wind scale, thereby increasing problem complexity. The resulting Figure 3.2 demonstrates the difference between the great circle distance (in blue) and optimal efficient flight path in the presence of wind (red). Wind is represented by overlaying blocks of wind (block size depending on the COAMPS scale) on the map, with blue representing a headwind and red representing a tailwind, see the color bar on the right. As intuition suggests, an optimal path takes advantage of a tailwind and avoids headwinds as demonstrated by the optimal red path in Figure 3.2.

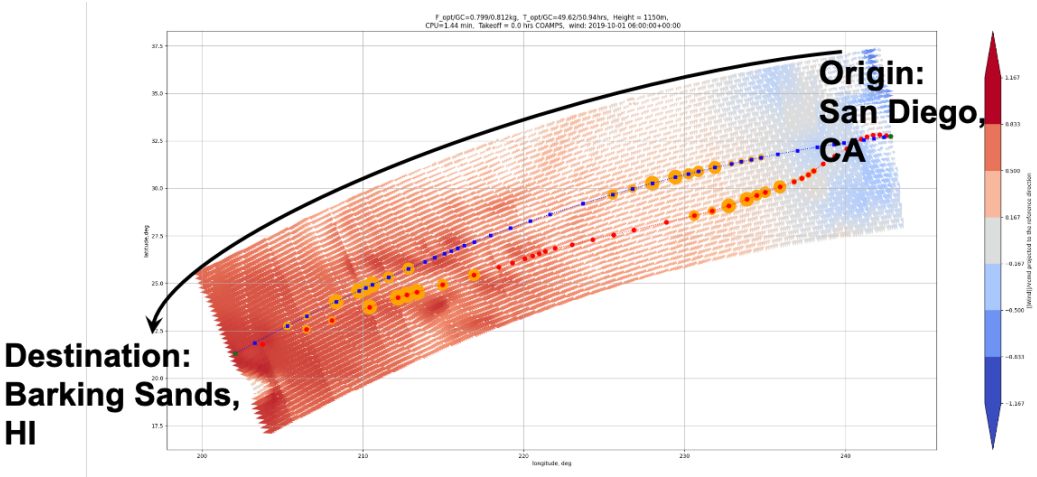

Figure 3.2. Comparison of the Great Circle Distance (Blue) and the Energy-Efficient (Red) Flight Paths in the Presence of Wind

CHAPTER 4:
The UAV Routing Model

4.0.1 Description

Our specialized vehicle routing model provides flexibility to the Marine logistician by minimizing the cost to deliver supplies from a depot to various "nodes" in the field. Every logistics support request, when tied to a geographic location and class of supply, becomes a node with associated constraints in our model. These requests, when prioritized, function as demands for our model to fill via a centralized supply depot with associated UAVs. We give the model flexibility to adapt to an infeasible solution by leaving certain demands unfulfilled.

By rewarding deliveries based on priority (routine, priority, or urgent) we encourage the model to find an optimal route that serves the maximum number of demand nodes prioritized by "importance," and satisfies those demands at the lowest overall energy cost.

4.0.2 Indices and Sets

Sets serve to identify groups of entities in our problem. Nodes are represented by the set n, indexed by i and j, while resupply UAVs are represented by the set m, indexed by k.

4.0.3 Data and Parameters

The cost matrix, built out with the boundary value problem solver, is the primary form of data for the UAV Routing Model. Of note, time and energy can be used interchangeably in this scenario because cost matrix C_{ijk}, represents the cost (in time or energy) of traveling from node i to node j by UAV k; it is understood that the specific choice of the metric represents a unique physical task while the formulation and implementation remain the same. Each demand node i also includes a demand D_i and a priority P_i. In order to fill these demands, a UAV must be able to transport some supply, S_k. Each UAV's payload defaults to a generic payload quantity, but can be customized by UAV type (heavy lift, medium, light, etc.).

Energy use by UAV k is calculated by using each UAV's total flight energy expended: $\sum_{i=1}^{n} \sum_{j=1}^{n} X_{ijk} C_{ijk}$. A "max energy" constraint ensures the UAV Routing Model routes do not exceed individual UAVs' energy capacities.

4.0.4 Decision Variables

The main family of decision variables is X_{ijk}, shown in Equation 4.1. This binary variable represents whether or not UAV k travels from node i to node j in order to meet node j's demand.

$$X_{ijk} = \begin{cases} 1, & \text{if UAV } k \text{ travels from node } i \text{ to node } j \\ 0, & \text{otherwise} \end{cases} \tag{4.1}$$

$$u_i \in \{\mathbb{Z}\} \qquad \forall i \in \{2, \ldots n\} \tag{4.2}$$

Our other family of decision variables is u_i, shown in Equation 4.2, which is used to prevent subtours (i.e., routes containing independent cycles that are not connected to a depot).

4.0.5 Objective Function

The UAV Routing Model's primary objective, as expressed in Equation 4.3, is to maximize the total reward obtained from making deliveries. R_j is the reward value at each node j and is based on priority of the demand with different values for routine, priority, and urgent requests. This tiered reward system ensures that the UAV Routing Model prioritizes requests based on need.

The second element of the objective function acts as a tie-breaker and ensures that, while we encourage the UAV Routing Model to complete all feasible deliveries, we also encourage the model to search for the minimum energy cost routing for those deliveries. The parameter ϵ influences how large the tiebreaker value is. Differences in scenario demand, distance between nodes, and weather conditions influence how important this term becomes since simpler resupply scenarios may have many feasible routes.

$$\max \sum_{i=1}^{n} \sum_{j:j>1,j\neq i} \sum_{k=1}^{m} X_{ijk} R_j - \epsilon \sum_{i=1}^{n} \sum_{j:j>1,j\neq i} \sum_{k=1}^{m} X_{ijk} C_{ijk} \tag{4.3}$$

4.0.6 Constraints

The core of our model is a VRP formulation based on the classical multiple-traveling salesman problem modified to include various other constraints important to the Marine logistician conducting UAV resupply operations.

Traveling Salesman Constraints

$$\sum_{j=2}^{n} X_{1jk} \leq 1 \qquad \forall\ k \in \{1, \ldots m\} \tag{4.4}$$

$$\sum_{i=2}^{n} X_{i1k} \leq 1 \qquad \forall\ k \in \{1, \ldots m\} \tag{4.5}$$

$$\sum_{j=1}^{n} \sum_{k=1}^{m} X_{ijk} \leq 1 \qquad \forall\ i \in \{2, \ldots n\} \tag{4.6}$$

$$\sum_{i=1}^{n} \sum_{k=1}^{m} X_{ijk} \leq 1 \qquad \forall\ j \in \{2, \ldots n\} \tag{4.7}$$

$$\sum_{i=1}^{n} X_{irk} = \sum_{j=1}^{n} X_{rjk} \qquad \forall\ r \in \{2, \ldots n\} \qquad \forall\ k \in \{1, \ldots m\} \tag{4.8}$$

$$u_i - u_j + (n-m) * \sum_{k=1}^{m} X_{ijk} \leq n - m - 1 \qquad \forall\ i, j \in \{2, \ldots n\} \qquad \forall\ k \in \{1, \ldots m\} \tag{4.9}$$

Constraints 4.4 and 4.5 ensure that every UAV that starts a delivery tour enters and exits the depot node only once; the depot is designated as node 1. Constraints 4.6 and 4.7 ensure that all non-depot nodes, if they are entered and exited, are only entered and exited once. Constraint 4.6 controls all incoming arcs to nodes, while 4.7 controls the exiting arcs from i to j. Constraint 4.8 ensures that the summation of all departures equals the summation of all entrances for each node and each UAV (i.e., if a UAV enters a node, it must also exit that

node). Constraint 4.9 is a Miller-Tucker-Zemlin subtour elimination constraint and ensures that degenerate subtours do not exist; see Miller, Tucker, and Zemlin (1960).

Capacity Constraint

$$\sum_{i=1}^{n} \sum_{j:j>1, j\neq i} d_j X_{ijk} \leq s_k \qquad \forall\ k \in \{1, \ldots m\} \tag{4.10}$$

The capacity constraint, Constraint 4.10, ensures that, for each UAV route, the total demand at all serviced nodes is less than or equal to the carrying capacity of the UAV (s_k).

UAV Performance Constraint

$$\sum_{i=1}^{n} \sum_{j:j>1, j\neq i} C_{ijk} X_{ijk} \leq EnergyMax_k \qquad \forall\ k \in \{1, \ldots m\} \tag{4.11}$$

Constraint 4.11 ensures that each UAV's energy consumption is less than or equal to that UAV's max on board energy capacity in watt-hours. This constraint ensures that each UAV's route does not exceed its performance bounds. Energy use is calculated using each UAV's energy consumed along arcs i and j. Each UAV's total energy use across the route is limited by its maximum energy capacity $EnergyMax_k$. In this model instance we assume that each UAV consumes energy at the same rate based on a generic UAV. Future developments in UAV technology will yield more accurate energy consumption data, which can be inserted into the model by UAV k.

4.0.7 Complete Formulation

Sets and Indices:

$i, j \in N = \{1, \ldots, n\}$ Nodes

$k \in M = \{1, \ldots, m\}$ UAVs

Data:

C_{ijk} = Energy for UAV k to travel from node i and node j [Watt-Hours]

d_j = Demand at node j [Pounds]

s_k = Capacity of UAV k [Pounds]

$EnergyMax_k$ = Energy capacity of UAV k [Watt-Hours]

ϵ = Penalty weight

R_j = Reward for delivering supplies to node j, based on demand priority

Decision Variables:

X_{ijk} = Binary variable representing whether or not UAV k travels along arc X_{ij}

u_i = Dummy variable to prevent degenerate subtours

$$\max \sum_{i=1}^{n} \sum_{j:j>1,j\neq i} \sum_{k=1}^{m} X_{ijk} R_j - \epsilon \sum_{i=1}^{n} \sum_{j:j>1,j\neq i} \sum_{k=1}^{m} X_{ijk} C_{ijk} \tag{4.12}$$

$$\sum_{j=2}^{n} X_{1jk} \leq 1 \qquad \forall\ k \in \{1,...m\} \tag{4.13}$$

$$\sum_{i=2}^{n} X_{i1k} \leq 1 \qquad \forall\ k \in \{1,...m\} \tag{4.14}$$

$$\sum_{j=1}^{n} \sum_{k=1}^{m} X_{ijk} \leq 1 \qquad \forall\ i \in \{2,...n\} \tag{4.15}$$

$$\sum_{i=1}^{n} \sum_{k=1}^{m} X_{ijk} \leq 1 \qquad \forall\ j \in \{2,...n\} \tag{4.16}$$

$$\sum_{i=1}^{n} X_{irk} = \sum_{j=1}^{n} X_{rjk} \qquad \forall\ r \in \{2,...n\} \quad \forall\ k \in \{1,...m\} \tag{4.17}$$

$$u_i - u_j + (n-m) * \sum_{k=1}^{m} X_{ijk} \leq n - m - 1 \quad \forall\ i,j \in \{2,...n\} \quad \forall\ k \in \{1,...m\} \tag{4.18}$$

$$\sum_{i=1}^{n} \sum_{j:j>1,j\neq i} d_j X_{ijk} \leq s_k \qquad \forall\ k \in \{1,...m\} \tag{4.19}$$

$$\sum_{i=1}^{n} \sum_{j:j>1,j\neq i} C_{ijk} X_{ijk} \leq EnergyMax_k \qquad \forall\, k \in \{1,...m\} \tag{4.20}$$

$$X_{ijk} \in \{0,1\} \qquad \forall i,j \in \{1,...n\} \tag{4.21}$$

$$u_i \in \{\mathbb{Z}\} \qquad \forall i \in \{2,...n\} \tag{4.22}$$

4.0.8 Model Output

When modeled in Python 3, using Pyomo and the solved with the CBC solver, the resulting output is a list of X_{ijk} tuples with a binary value of one shown in Figure 4.1. These tuples denote the flight path of the individual UAVs across the graph. The UAV flight path is shown visually on the graph in Figure 4.2.

A typical run of the UAV Routing Model with 21 demand nodes defines 1,378 constraints and 1,474 binary variables. Depending on the number of UAVs, limitations on UAV carrying and energy capacity, and priorities of the demands, a complete run takes between one and ten minutes of computation time to solve with a 2.9 GHz Intel Core i9 CPU with 32 GB of RAM.

```
(1, 4, 1)
(2, 1, 1)
(3, 2, 1)
(4, 5, 1)
(5, 6, 1)
(6, 11, 1)
(7, 3, 1)
(8, 7, 1)
(9, 8, 1)
(10, 14, 1)
(11, 10, 1)
(12, 9, 1)
(13, 12, 1)
(14, 15, 1)
(15, 16, 1)
(16, 20, 1)
(17, 13, 1)
(18, 17, 1)
(19, 18, 1)
(20, 22, 1)
(21, 19, 1)
(22, 21, 1)
```

Figure 4.1. Sample Output of the UAV Routing Model in the Form: (Node i, Node j, UAV k)

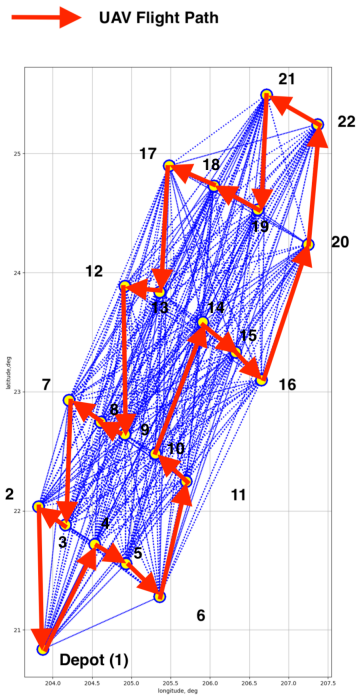

Figure 4.2. Resulting Flight Path on the 21-Demand-Node Graph

CHAPTER 5:
Real World Application

This chapter describes the results of the two-tiered optimization of UAV flight paths and routing using real-world mesoscale wind forecasts from COAMPS and geographic data off the eastern coast of Maui, Hawaii.

5.1 Distance as a Metric

In order to test the UAV routing model with an asymmetric cost matrix based on real-world wind data, we developed a ten-node scenario off of the Hawaiian coast. This functioned as a proof-of-concept for our two-tiered optimization method, combining the cost matrix from the boundary value problem with the UAV Routing Model's multiple-traveling salesman optimization.

Our first test, using 10 delivery nodes with "routine" delivery priorities shown in Figure 5.1, compares the energy consumption from the UAV Routing Model with the distance results from a shortest path model only using great circle distances between nodes.

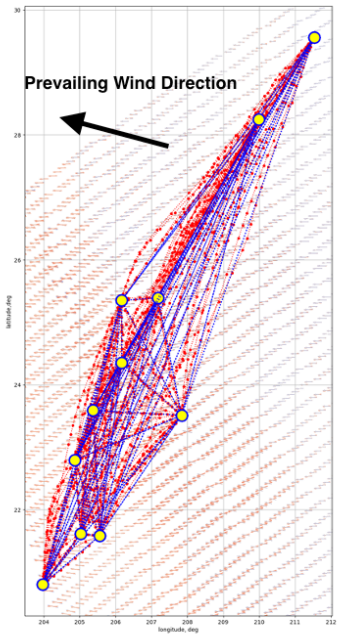

Figure 5.1. 10-Node Graph with Great Circle Distances in Blue and Optimal Energy Efficient Flight Paths in Red. COAMPS wind field is overlaid in background.

With the wind-based cost matrix there are dramatic differences between energy use with travel from i to j and j to i. These differences account for the presence of headwinds, which make certain arcs impassable or nearly impassable, as shown in Figure 5.2. This difference is significant because it proves the impact that wind has on UAV energy consumption along specific arcs of travel. The direction of travel, irrelevant with a symmetric cost matrix based simply on distance, becomes critical in the real world in order to achieve minimum energy expenditures across the deliveries. We acknowledge that the minimum-energy model is not guaranteed to provide the minimum-time solution because the optimal trajectories will likely (in the presence of head winds) deviate from the great circle path, which will result in longer flight distance, and can result in a longer flight time.

```
(13, 15) : 27602.66
(15, 13) :  8454.72
```

Figure 5.2. The Actual Energy Cost, (Wh) Depending on Direction of Travel, Along the Arc from Node 13 to Node 15

Our ten-node scenario saw a longer flight time (using a nominal UAV speed of 15 m/s), and a longer flight distance in the minimum energy routing model. Since airspeed is one of the two control inputs to the boundary value problem, and due to the differences between great circle distance and the optimal trajectories, this comparison is rudimentary, but it does show that we were able to achieve the same delivery result using 2.5 percent less energy. It is worth noting that the real energy savings could be significantly higher, which is suggested by the data in Figure 5.2. We could not account for real-world energy consumption using the distance-only method since it did not occur in the presence of actual weather conditions. These results, despite the shortcomings of a direct comparison, show that our method saves energy.

Though the gains are relatively small, they show that our method does improve the time duration and the energy efficiency in this scenario. We hypothesize that large time differences were not observed in this specific instance due to small wind intensity and the alignment of the delivery nodes in a linear pattern. This linear pattern means that there are simply less options for the model to choose from that would avoid headwinds, since we still mandate that all nodes are supported.

5.2 Maui Resupply Scenarios

We further tested the UAV Routing Model with a scenario off of the Hawaiian coast where a supply ship must conduct resupply operations for 14 "routine" demands with three UAVs for ships clustered in three locations, shown in Figure 5.3 and represented by the graph in Figure 5.4. We limit the three assigned UAVs to only be able to support a maximum of five deliveries by adjusting their maximum carrying capacity, but do not limit their flight time.

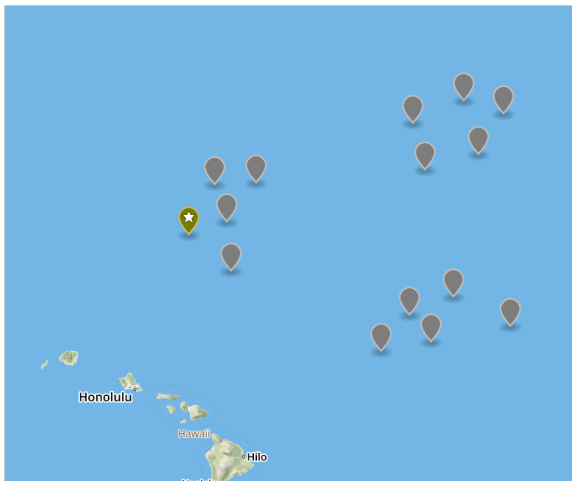

Figure 5.3. Geographic Representation of 15-Node Scenario with the Depot Node Represented by a Star

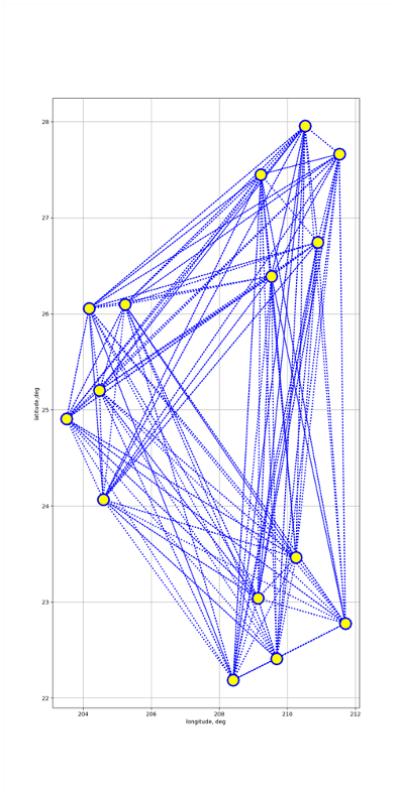

Figure 5.4. Resulting Graph from the 15-Node Scenario

These results, shown in Figure 5.5, are meaningful in two ways: they show UAVs tackling

groups of demands in order to minimize total energy expenditures over the graph, and they show UAVs moving through the head wind to serve early nodes, and then returning to the depot node using tail winds. As the asymmetric cost matrix shown in Figure 5.2 demonstrates, direction matters and the UAV Routing Model takes advantage of the differences.

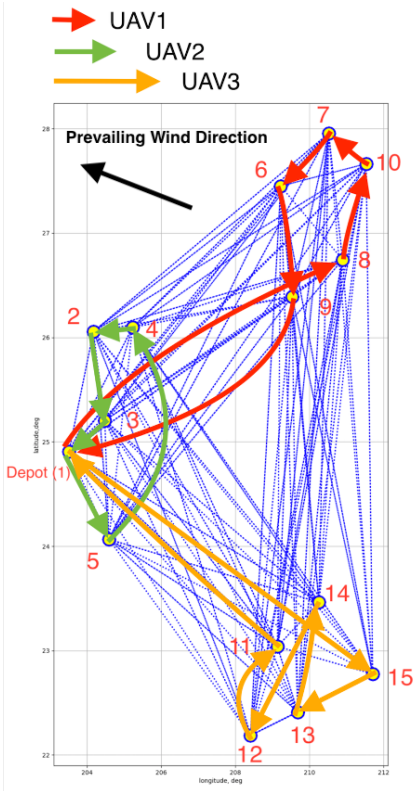

Figure 5.5. UAV Routing to 14 "Routine" Demand Nodes

For the second scenario, we test the UAV routing model's ability to accommodate higher priority requests by changing five requests from "routine" to "urgent" priority. This scenario represents higher supply consumption by a particular group of units due to combat or operational tempo. We further limit the UAVs' ability to supply demand nodes by ensuring that the UAVs can only fulfill five total demands. Running this scenario through the UAV Routing Model shows the UAVs fulfilling the five "urgent" requests, while ignoring the routine requests. Figure 5.6 shows the UAV flight paths through the graph, again demonstrating early movement through headwinds in order to take advantage of tailwinds to return to the depot.

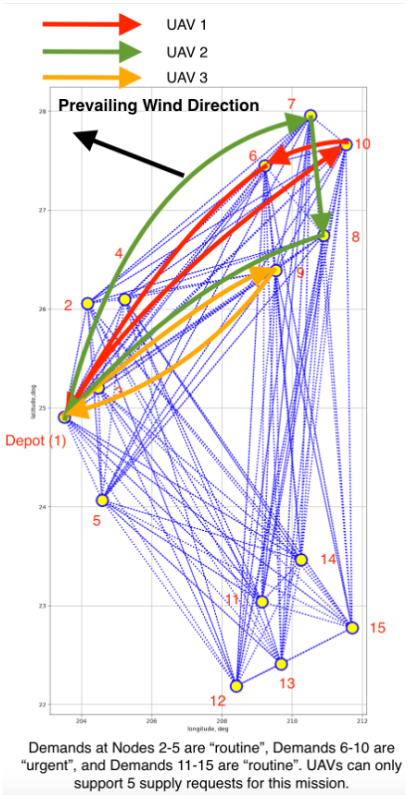

Figure 5.6. UAV Routing to 5 "Urgent" Demand Nodes

Our final scenario uses a new layout of 21 demand nodes and one depot node located on the island of Maui. The nodes requesting supply deliveries are arrayed in lines, with COAMPS wind data overlaid, and are shown in Figure 5.7. We chose this scenario because the optimal routing solution isn't immediately obvious to a human, even when the prevailing wind direction is labeled, since there are no clear groups of nodes that can be easily supported from the depot node.

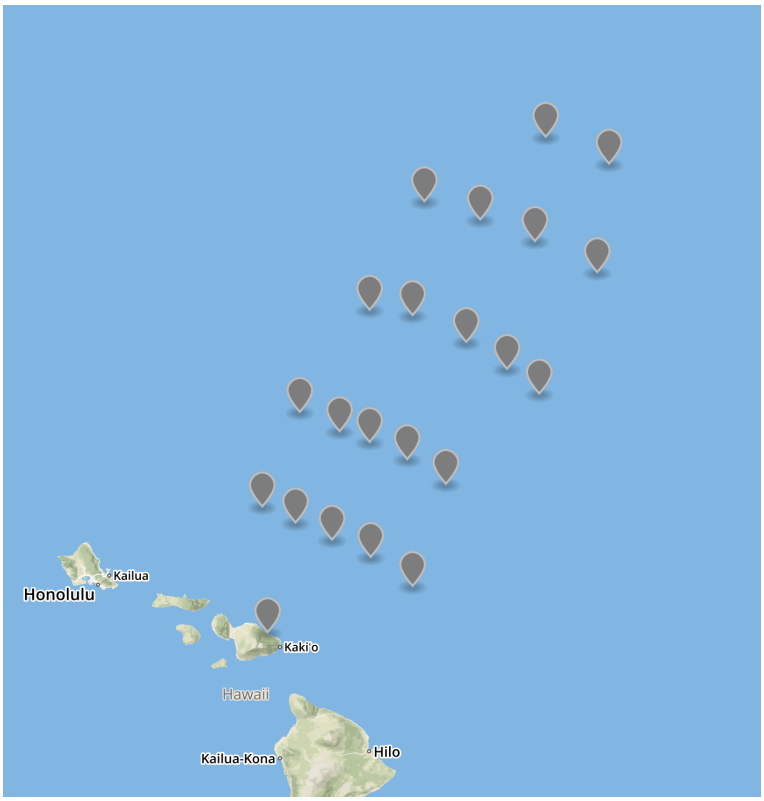

Figure 5.7. Geographic Representation of the Maui Resupply Scenario with 21 "Routine" Priority Demand Nodes (Depot Node on the Island of Maui)

Once optimal flight paths are calculated, the resulting Figure 5.8 shows the connecting great circle arcs between all of the nodes in blue, with optimal trajectories shown in red based on the flight path results from the flight path optimization. We limit the three UAVs so that they can only support 7 of the 21 individual node demands per UAV by adjusting their maximum weight capacity, before using The UAV Routing Model to identify optimal routing for all three UAVs.

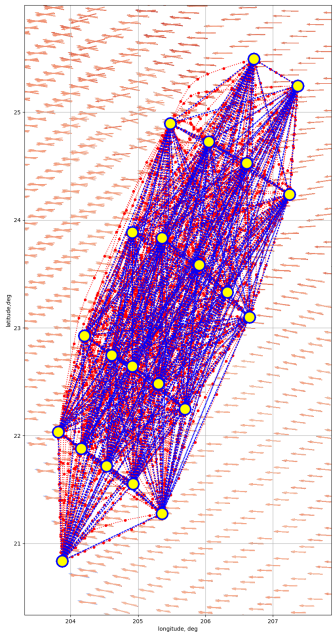

Figure 5.8. Great Circle (Blue) and Optimal Flight Path (Red) Graph from 21 Demand Node Scenario

Figure 5.9 shows the final routing results by UAV k. Comparing this optimal result to two alternative possible routes through the graph, which were created by going backwards along the optimal paths (instead of $1 \rightarrow 2 \rightarrow 3 \rightarrow 1$, travel from $1 \rightarrow 3 \rightarrow 2 \rightarrow 1$) and attempting to pick an optimal route without the help of a computer, the optimal routing resulted in energy savings of between 2.5 percent and 11 percent. These final results illustrate the value of combining the boundary value problem's indirect method and the UAV Routing Model to identify three UAV routes that are the most energy efficient and deliver supplies to all 21 demand nodes. These routes would not be immediately evident to a logistician in charge of conducting resupply operations on the ground, but they do follow a similar pattern to our previous results. They start by flying along the shortest legs to the most distant node against head winds early on in order to reap energy gains of a tailwind along the longest return route back to the supply depot.

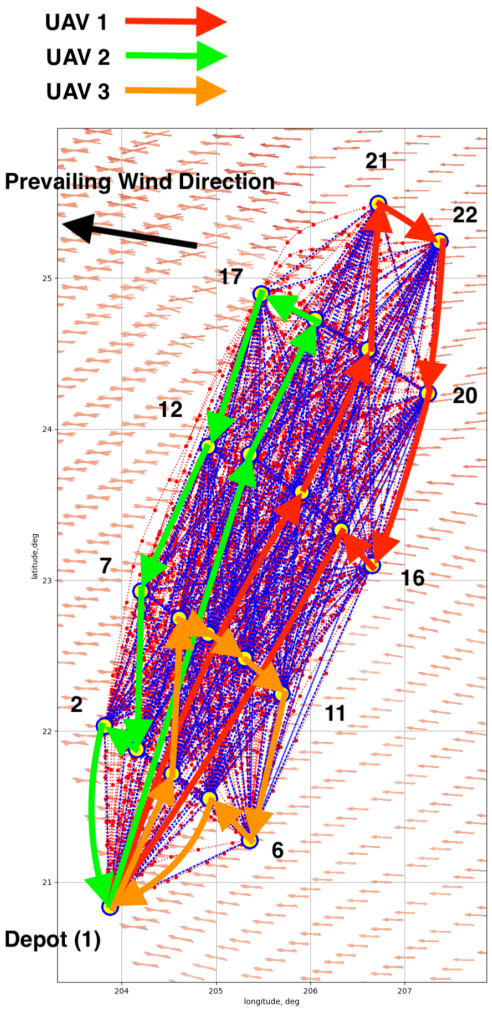

Figure 5.9. Resulting Optimal Routing Graph from 21 Demand Node Scenario

THIS PAGE INTENTIONALLY LEFT BLANK

CHAPTER 6:
Conclusions / Recommendations

6.1 Conclusion

This thesis demonstrates the value in combining direct and indirect optimization methods to model real-world weather conditions and solve for optimal UAV routing. Gains in energy efficiency translate to gains in range, carrying capacity, and decreases in energy required to fulfill mission requirements. These decreases mean a lower logistical burden on Marines as they conduct EABO in harm's way.

Our model also shows the benefit of allowing Marines to prioritize requests based on need and urgency by using three commonly used demand tiers ("routine", "priority", and "urgent"). By maximizing the reward value in the objective function of the UAV Routing Model differently for different demands, we are able to better serve Marines on the ground by ensuring that "urgent" requests are supported before the model supports more "routine" requests. In combat, with varying demands based on real world factors, this can mean the difference between mission success or failure as Marines contend with supply shortages that depend on the intensity of combat at their dispersed bases.

6.2 Future Work

Optimal routing has many different offshoots, but the most meaningful future work in the topic discussed in this thesis center around scheduling, flexibility, UAV resource allocation, and computational efficiency. These four subjects all have a tangible impact on Marines on the ground.

The UAV Routing Model did not address specific delivery time windows. Developing the capacity for time window specific delivery requests mean that Marines can choose when they need resources delivered, which can better align with their battle rhythm based on operational tempo.

Analyzing the UAV Routing Model can yield insights into optimal resource allocation. By

developing the model to support multiple depots we can better understand where to establish supply depots to optimally support Marines at dispersed bases. A design of experiments matrix could support this offshoot by identifying key factors in the establishment of supply depots capable of supporting complex UAV resupply operations

The UAV Routing Model could also be further developed by adding flexibility to the delivery options. If a UAV is allowed to partially fulfill a delivery, and multiple UAVs are allowed to deliver to a requesting node, then that node could be serviced rather than dropped.

Improvements could also improve the computational efficiency for both the boundary value problem and the UAV Routing Model. More research could be done to improve model reward and tie breaker scaling based on the data from the BVP. These improvements would allow the program to run faster on the laptops that Marines currently carry in the field.

6.3 Final Thoughts

In a future fight against a near-peer enemy, Marines must be ready to operate in austere conditions at expeditionary bases with contested airspace overhead. The nature of future operations means establishing bases in dispersed locations without clear supply lines. Using autonomous UAVs to conduct resupply operations is a future necessity because high value equipment and Marines cannot be quickly replaced.

This thesis shows the value of using real-world wind when identifying the cost matrix for resupply routes to support Marines making prioritized supply requests. Combining this realistic data with a multiple-traveling salesman-style routing system yields routing results that would not be evident to a task saturated logistician short on time. These optimal routing results save energy, energy that can be used to increase UAV range, carry more supplies, and limit the energy burden at supply nodes far from America's shores.

List of References

Bryson, A. E. (1975). *Applied optimal control: Optimization, estimation, and control* (Rev. printing. ed.). Washington, D.C.: Hemisphere PubCorp; New York: Halsted Press.

Cheng, C., Adulyasak, Y., & Rousseau, L.-M. (2018). *Formulations and Exact Algorithms for Drone Routing Problem*. Centre Interuniversitaire de Recherche sur les Réseaux d'Entreprise, la Logistique et le Transport (CIRRELT), Montreal, Canada.

Dobrokhodov, V., Jones, K. D., Walton, C., & Kaminer, I. I. (2020). Energy-optimal trajectory planning of hybrid ultra-long endurance UAV in time-varying energy fields. In *AIAA scitech 2020 forum.* American Institute of Aeronautics and Astronautics. Retrieved 09 April 2020, from https://arc.aiaa.org/doi/abs/10.2514/6.2020-2299 (_eprint: https://arc.aiaa.org/doi/pdf/10.2514/6.2020-2299) doi: 10.2514/6.2020-2299

Dorling, K., Heinrichs, J., Messier, G., & Magierowski, S. (2016). *Vehicle Routing Problems for Drone Delivery*. Retrieved 22 November 2019, from http://search.proquest.com/docview/2079676585/?pq-origsite=primo doi: 10.1109/TSMC.2016.2582745

Driscoll, N. R. (1967). *Effects of a simple stability augmentation system on the performance of non-instrument-qualified light-aircraft pilots during instrument flight* (Tech. Rep.). National Aeronautics and Space Administration (NASA), Washington, D.C.

Hart, W. E., Laird, C. D., Watson, J.-P., Woodruff, D. L., Hackebeil, G. A., Nicholson, B. L., & Siirola, J. D. (2017). *Pyomo–optimization modeling in python* (Second ed., Vol. 67). Springer Science & Business Media.

Hart, W. E., Watson, J.-P., & Woodruff, D. L. (2011). Pyomo: Modeling and solving mathematical programs in python. *Mathematical Programming Computation*, *3*(3), 219–260.

Jaillet, P., & Lu, X. (2011). Online traveling salesman problems with service flexibility. *Networks*, *58*(2), 137-146.

Kaempfer, Y., & Wolf, L. (2019). Learning the multiple traveling salesmen problem

with permutation invariant pooling networks. Retrieved 06 Febuary 2020, from http://arxiv.org/abs/1803.09621

Liu, Z., Sengupta, R., & Kurzhanskiy, A. (2017). A power consumption model for multi-rotor small unmanned aircraft systems. In *2017 international conference on unmanned aircraft systems (ICUAS)* (pp. 310–315). IEEE. Retrieved 23 February 2020, from http://ieeexplore.ieee.org/document/7991310/ doi: 10.1109/ICUAS.2017.7991310

Marinova, P. (2012). *Determination of an area avoidance wind optimal trajectory by the methods of optimal control* (Thesis). Department of Mathematics, University of Hamburg.

Miller, C. E., Tucker, A. W., & Zemlin, R. A. (1960). Integer programming formulation of traveling salesman problems. *J. ACM*, *7*(4), 326–329. Retrieved from https://doi.org/10.1145/321043.321046 doi: 10.1145/321043.321046

Nachmani, G. (2007). *Minimum-energy flight paths for UAVs using mesoscale wind forecasts and approximate dynamic programming* (Thesis). Retrieved 22 November 2019, from http://bosun.nps.edu/uhtbin/cgisirsi.exe/Thu+Nov+06+09:01:34+2008+/SIRSI/0/520/07Dec_Nachmani.pdf

National Security Council (NSC). (2017). *National security strategy of the united states of america.* National Security Council. Retrieved from https://www.whitehouse.gov/wp-content/uploads/2017/12/NSS-Final-12-18-2017-0905.pdf

Ozdamar, L. (2011). Planning helicopter logistics in disaster relief. *OR Spectrum*. Retrieved from https://www.researchgate.net/publication/225640127_Planning_helicopter_logistics_in_disaster_relief/link/5485814f0cf24356db60f4f0/download doi: 10.1007/s00291-011-0259-y

Pontryagin, L. S. (1962). *The mathematical theory of optimal processes*. Geneva, Switzerland: Interscience Publishers.

The Naval Research Laboratory. (1997). *The naval research laboratory's coupled ocean/atmosphere mesoscale prediction system (coamps®)* (Tech. Rep.). The NRL. Retrieved from www.nrlmry.navy.mil/coampsweb/web/home

United States Marine Corps (USMC). (2016). *Marine corps operating concept.* United States Marine Corps. Retrieved from https://www.mcwl.marines.mil/Portals/34/Images/MarineCorpsOperatingConceptSept2016.pdf

Initial Distribution List

1. Defense Technical Information Center
   Ft. Belvoir, Virginia

2. Dudley Knox Library
   Naval Postgraduate School
   Monterey, California